Volume 6 No. 1, Feb 2018

Transactions on Networks and Communications

ISSN: 2054-7420

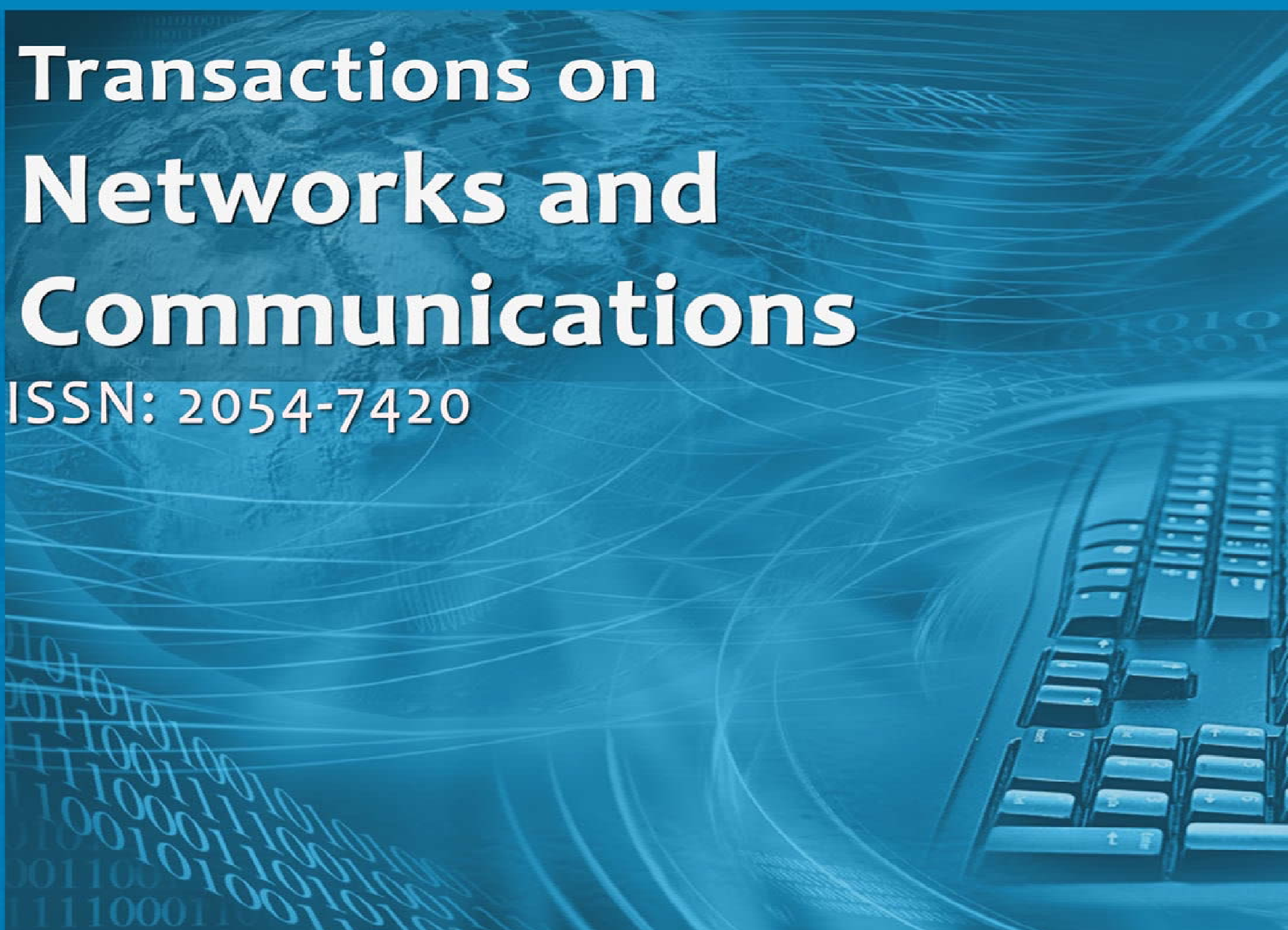

Society for Sciences and Education - United Kingdom

TABLE OF CONTENTS

EDITORIAL ADVISORY BOARD

DISCLAIMER

All the contributions are published in good faith and intentions to promote and encourage research activities around the globe. The contributions are property of their respective authors/owners and the journal is not responsible for any content that hurts someone's views or feelings etc.

SOCIETY FOR SCIENCE AND EDUCATION
UNITED KINGDOM

TNC TRANSACTIONS ON NETWORKS AND COMMUNICATIONS

VOLUME 6, NO. 1
ISSN: 2054 -7420

Performance Evaluation of Multi-hop Wireless HART Network on a Real-life Testbed

Kaleab Worku[1], Jacob Hupp[2], Tirthankar Ghosh[2], Yi Zheng[2]
[1]*Department of Computer Science and Information Technology*
St. Cloud State University, St. Cloud, Minnesota, USA
[2]*Department of Electrical and Computer Engineering*
St. Cloud State University, St. Cloud, Minnesota, USA
tghosh@stcloudstate.edu

ABSTRACT

Advances in WirelessHART standard in industrial control systems have led to performance evaluation and security analysis in both real-world testbeds as well as in controlled lab environments. We have conducted months-long experiments with WirelessHART network in a multi-hop setting in our laboratory. Latency, stability, and reliability have been used as metrics to measure performance of individual links and the overall network for five hops and seven hops. We have deliberately deviated from following the best practices in designing the topology to study network performance under strained conditions. In addition to using metrics as defined in WirelessHART literature, we have also studied network stability over multiple hops with single paths. Our findings show that having at least one low stability link can have an impact on multihop stability, while still maintaining a very high overall network reliability of 99.98% or higher. Details of the experiment along with results and lessons learned are presented in the paper.

Keywords—Wireless HART, performance analysis

ACKNOWLEDGMENT

We sincerely express our gratitude to all students who worked on the project, especially Vinicius Binotti, Yanik Kientega, and Robert Finstad who were involved with the initial set up. We thank Arthur Tiam, Zachary Wild, and Hilton Bannerman-Williams for developing the SmartMote system. We are grateful to Emerson Process Management for providing us funds to conduct these experiments and study

1 Introduction

WirelessHART is a wireless sensor networking standard designed for industrial control systems. The protocol is standardized by the HART Communication Foundation [2], and provides an alternative solution for Bluetooth and ZigBee, in noisy environments [1, 5]. WirelessHART was designed to create a wireless protocol solution for the already existing HART protocol [9], which is the most common protocol for field devices. The standard is based on IEEE 802.15.4 [10]. It utilizes a time synchronized, self-organizing, and self-healing mesh architecture, forming full mesh network topologies. This kind of networks contains a

DOI: 10.14738/tnc.61.3836
Publication Date: 20th December 2017
URL: http://dx.doi.org/10.14738/tnc.61.3836

large number of nodes (henceforth referred as motes), which normally uses batteries as a power source and organize themselves into a multi-hop wireless network. The network uses medium access control (MAC) technique [2] for successful operation. MAC protocol avoids collisions of data transmitted by assigning a time for each mote on the network.

WirelessHART is a global IEC-approved standard (IEC 62591) [3] that specifies an interoperable self-organizing mesh technology in which field devices form a wireless network that dynamically mitigate obstacles in the process environment. The WirelessHART field networks (WFN) communicate data back to host systems securely and reliably, and can be used for both control and monitoring applications. The similarities between traditional HART and WirelessHART allow end users to leverage training of existing process organizations when adopting WirelessHART. In addition, the reduced installed cost of WirelessHART extends the benefits of automation to end user applications that previously were out of reach since they could not justify the costs associated with typical wired capital projects. The opportunity for long-term benefit makes it compelling for users to expand process manufacturing project planning to evaluate the impact of WirelessHART on maintenance, safety, environment, and reliability. Additionally, by removing the physical constraints of wiring and power as well as reducing weight and space, wireless networks increase flexibility in project execution, providing solutions that can mitigate risk and improve project schedules. Its standard is a secure networking technology that operates in the 2.4GHZ ISM radio band and utilizes IEE 802.15.4 [4]. WirelessHART protocol communications are precisely scheduled using an approach referred to as Time Division Multiple Access (TDMA). This scheduling is performed by the network manager, a device that is the central component of the mesh network architecture. Most of the research conducted in Wireless HART networks focused on scheduling at the MAC layer, and

designing frames for communications between motes and between motes and manager. Not much research was conducted to study performance of such networks over multiple hops in a real-world testbed. In [8] the authors performed a laboratory experiment on a wide scale deployment of wireless HART network over a period of 120 hours, and monitored packet loss, latency, and reliability. Their deployed network achieved a near 100% reliability, with very low packet loss and latency. However, as the experiment was conducted for only 120 hours, it fails to provide a long-term performance evaluation of the network as a whole and the stability of links in particular.

In this paper, we have presented results from a months-long study of wireless HART network deployed in our laboratory. The study was mainly focused on measuring performance of links over multiple hops and also the network as a whole with a network configuration that deviates significantly from the standard industry practices. Detailed experimental setup and results are discussed in the subsequent sections.

2 Method and Experimental Setup

The experiment was carried out in two phases. In the first phase, a five-hop topology was deployed in the Integrated Science and Engineering Laboratory Facility (ISELF) building on our campus, as shown in Fig 1 below. Nine motes were used in the experiment, these motes are from Linear Technology [6]. The topology was designed and deployed in a way that the farthest mote has a five-hop path to the network manager. We emphasize that we have deliberately deviated from following the best topological practices followed in industry to study the network performance under strained conditions, and implemented only single paths in the configuration. The topology spans across two floors in the ISELF building, with approximately 450 square meters per floor. The experiment was conducted for two-and-half months. Following five-hop routes were formed:

Route 1: network manager -> 57 -> C2 -> 6B -> 05 -> 11

Route 2: network manager -> FC -> 8D -> BA -> DE -> 11

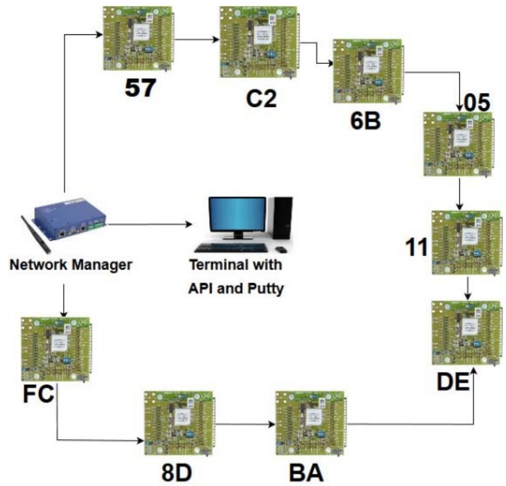

Figure. 1. Five-hop topology

In the second phase, a seven-hop topology was set up in the same building, as shown in Fig 2 below. Eight motes were used, including a mote designed by the Electrical Engineering students. This mote is a SmartMote system which integrates WirelessHART and embedded components to collect measurements from atmospheric sensors [7]. The system can join or exit an existing system without additional programming device. The SmartMote system also has solar powered batteries and is designed for easy configuration by users. It measures luminosity, temperature and humidity. The topology was designed and deployed in such a way that the farthest mote has a seven-hop path to the network manager. Once again, we deviated from topological best practices on purpose. The experiment was conducted over a period of one month.

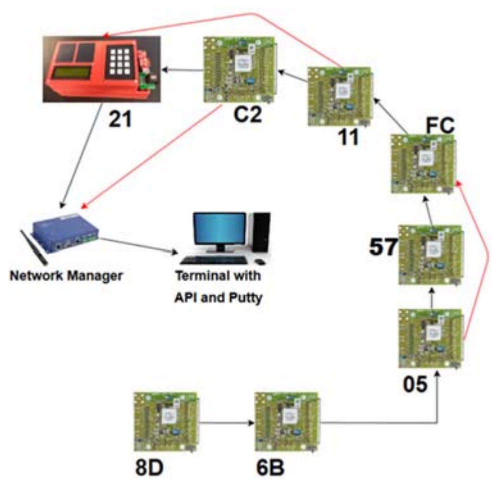

Figure. 2. Seven-hop topology

3 Results and Analysis

In the following sections, results from our five-hop and seven-hop experiments were discussed in details.

3.1 Five-hop experiment

Nine motes and a network manager were used for this experiment. Three parameters, as defined in the WirelessHART literature, were used to measure the network performance: latency (in milliseconds), stability (in percentage) and reliability (in percentage). In addition, we studied the multihop stability of the five-hop path based on individual link stability values. Due to the distance and obstacles among the motes and the network manager, latency, stability and reliability varied in each link. Average values were recorded for all three measurements throughout the network. Fig 3 shows a screenshot from the Application Programming Interface, with all motes being operational, the first device shown is the network manager.

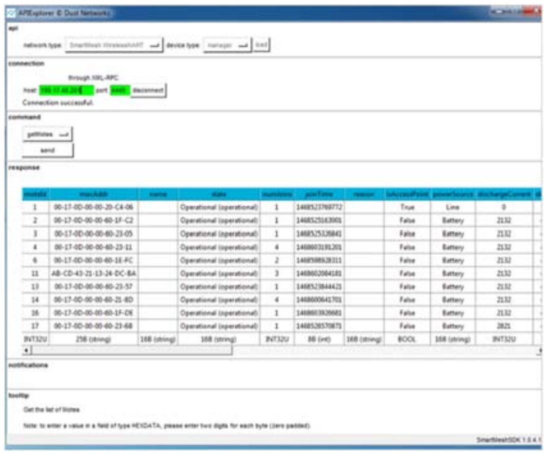

Figure. 3. API showing motes' status

Latency

Latency is the average time required for a data packet to travel from the originating mote to the manager. Latency also varies in each link across the network, and the value represents average network latency. The network manager calculates latency for each packet by subtracting the time when the packet was received from the packet timestamp in the network layer header, which indicates when the packet was generated or accepted by the mote.

The formula to calculate latency is:

$$L_{ij} = T_r - T_s \quad (1)$$

Where, L_{ij} = latency for link connecting motes i to j

T_r = Time packet received

T_s = Time packet sent

$$L_{avg} = \frac{1}{n} * \sum_{1}^{n} L_{ij} \quad (2)$$

Where, L_{avg} is the average latency for the whole network

L_{ij} is latency of each hops (links)

n is the number of hops (links)

Figure 4 below shows a screenshot showing latency, number of packets generated, lost, and duplicated.

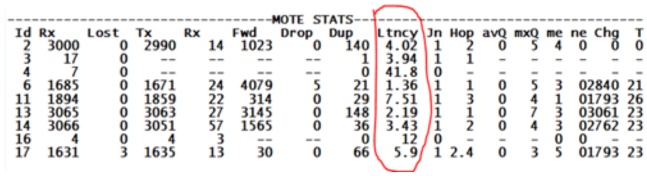

```
-----------------------------------MOTE STATS-----------------------------------
Id Rx     Lost  Tx     Rx     Fwd    Drop   Dup   Ltncy Jn Hop avQ mxQ me ne Chg   T
 2  3000     0  2990     14   1023      0   140  4.02  1   2   0   5  4  0     0  0
 3    17     0    --     --     --     --     1  3.94  1   1   -   -  -  -     -  -
 4     7     0    --     --     --     --     0  41.8  0   -   -   -  -  -     -  -
 6  1685     0  1671     24   4079      5    21  1.36  1   1   0   5  3  02840  21
11  1894     0  1859     22    314      0    29  7.51  1   3   0   4  1  01793  26
13  3065     0  3063     27   3145      0   148  2.19  1   1   0   7  3  03061  23
14  3066     0  3051     57   1565      0    36  3.43  1   2   0   4  3  02762  23
16     4     0     4      3     --     --     0    12  0   -   -   -  0  0     -  -
17  1631     3  1635     13     30      0    66   5.9  1 2.4   0   3  5  01793  23
```

Figure. 4. Latency values

Latency increases with distance between motes and the network manager. Latency can be decreased by decreasing the number of hops or by decreasing the distance between the network manager and the motes. Table 1 below summarizes average latencies observed for each hop for both five-hop paths.

Table 1: Latency values for paths with varying hops

Number of Hops	Latency (in Seconds)
1-hop Latency	1.590301282
2-hop Latency	2.607154461
3-hop Latency	2.994113637
4-hop Latency	5.357397018
5-hop Latency	6.026492308

Stability

Stability is the average percentage of packets that were acknowledged by the MAC layer recipient. Stability is calculated in different places in the network. It is calculated between motes (link to link), between mote and network manager, and the average stability for the whole network. The formula to calculate stability between motes (link to link) or between a mote and the network manager is:

$$S_{ij} = 100 * \frac{T_{ackp}}{T_{spk}} \quad (3)$$

Where, S_{ij} is stability between mote i and mote j (link to link)

T_{spk} is Total packets sent

T_{ackp} is Total acknowledged packets

Formula to calculate average stability is:

$$S_{avg} = \frac{1}{n} * \sum_{i=1}^{n} S_{ij} \quad (4)$$

Where, S_{avg} is average stability for the whole network

S_{ij} is stabilities of each hops (link) in the network

n is the number of hops (links)

If a mote sends a packet to another mote, but fails to receive an acknowledgment from the destination, the sender mote assumes that the packet is lost. Fig 5 is a screenshot of path stability values.

--------------------------------PATH STATS--------------------------------

MoteA	MoteB	ABPower	BAPower	ABTx(Fail)	ABRx	BATx(Fail)	BARx	Stab.
1	6	-73	-76	0(0)	737	9602(2539)	7284	73.56%
1	13	-76	-81	0(0)	298	14k(7353)	8117	50.98%
2	13	-74	-76	7162(1821)	1002	0(0)	180	74.57%
2	17	-60	-68	0(0)	168	3949(300)	2400	92.4%
6	14	-80	-84	0(0)	193	10k(4861)	583	54.33%
11	14	-82	-85	5580(2757)	782	0(0)	99	50.59%
13	17	-84	-85	0(0)	140	4141(2565)	1638	38.06%

Figure. 5. Stability values

The first two rows show the stability between the network manager and two motes that are directly connected to the manager which is labeled as 1; the stability values are respectively 73.56% and 50.98%. The rest of the lines show stability between motes. Stability varies from link to link, the variation is attributed to the locations of the motes and obstacles between them. Looking at the last line in Fig 5 above, it can be seen that the stability value between motes 13 and 17 is only 38.06%, which is attributed to the fact that the two motes are placed in different floors with mote 2 between them. However, motes 13 and 17 were occasionally able to connect with each other and transfer packets. Looking at the figure again, stability values between motes 2 and 13 and between 2 and 17 are 74.57% and 92.4% respectively, which shows that stability is inversely proportional to the distance between motes. Tables 2 and 3 below summarize stability values for each hop-path for both routes. Table 4 summarizes the average stability values for both routes over each-hop path.

Table 2: Average stability values for route1

Number of Hops	Stability
1 hop average Stability	37.53%
2 hops average Stability	54.34%
3 hops average Stability	65.73%
4 hops average Stability	67.24%
5 hops average Stability	65.13%

Table 3: Average stability values for route 2

Number of Hops	Stability
1 hop average Stability	78.3%
2 hops average Stability	71.91%
3 hops average Stability	67.83%
4 hops average Stability	75.43%
5 hops average Stability	76.42%

Table 4: Average stability values combining routes 1 and 2

Number of Hops	Stability
1 hop average Stability	57.915%
2 hops average Stability	63.125%
3 hops average Stability	66.78%
4 hops average Stability	71.335%
5 hops average Stability	70.775%

Reliability

Reliability is the percentage of data packets transmitted by motes that the network manager actually received. The manager calculates reliability by dividing the number of packets it received by the sum of number of packets received and packets lost. The reported values are network averages.

$$R = 100 * \frac{U_{pkr}}{T_{pkg}} \tag{5}$$

Where, R is reliability of the network

T_{pkg} is Total packets generated

U_{pkr} is Unique Packets received, offsetting duplicate packets received

Figure 6 below shows reliability value for one snapshot of time. As can be seen from Fig 6, reliability is 99.98% which means 99.98% of the packets generated have reached their destination irrespective of number of retransmissions. Here, the network manager computes reliability only for its one-hop motes.

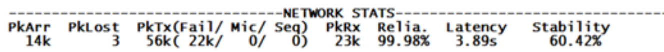

```
--------------------------------NETWORK STATS--------------------------------
PkArr  PkLost  PkTx(Fail/ Mic/ Seq)  PkRx  Relia.  Latency  Stability
 14k       3    56k( 22k/   0/   0)   23k  99.98%   3.89s     60.42%
```

Figure. 6. Reliability values

Multihop Stability

In our experiments we have computed multihop stability based on the probability of link failure, which in turn is based on individual link stability, as below:

$$R_{sd} = \prod_{\substack{i=s \\ j=s+1 \\ i \neq j}}^{\substack{d \\ d-1}} S_{ij} \tag{6}$$

Where, Rsd = Multihop stability between motes s and d

Sij = Stability value between motes i and j

We computed multihop stability values at different times of days during the entire period of the experiment. Table 5 below shows these values for our five-hop experiment for both routes 1 and 2.

Table 5: Multihop stability for five-hop experiment

Discrete time slots	Multihop Stability – Route 1 (in percentage)	Multihop stability– Route 2 (in percentage)
1	8.2	18.75
2	8.2	23.81
3	9.6	33.35
4	9.6	7.53
5	10.5	33.58

Following screenshots in Fig 7 were captured in 15 minutes’ interval to evaluate the network performance.

```
It is now .................. 07/06/16 10:41:03.
This interval started at ... 06/27/16 14:03:18.

-------------------------------NETWORK STATS---------------------------------
PkArr  PkLost  PkTx(Fail/ Mic/ Seq)  PkRx  Relia.  Latency   Stability
 215k      10 1147k(471k/   0/   0)  369k    100%   3.38s      58.93%

--------------------------------MOTE STATS-----------------------------------
 Id Rx     Lost  Tx     Rx     Fwd    Drop  Dup    Ltncy Jn Hop avQ mxQ me ne Chg  T
  2   28k     5   28k   271    20k     15  1322   3.71  1   2   0    5 70  0 14k 24
  4   21k     1   21k   369    132      4   791   5.94 19 3.9   0    5 36 361017 24
  6   15k     0   15k   448    71k      5   279   0.55  1   1   0    6 71  0 21k 21
 11   28k     0   28k   394    30k      0   528   2.91  3   3   0    5 60  01766 26
 13   28k     0   28k   410    48k     14  1340   1.91  1   1   0    7 74  0 25k 23
 14   28k     0   28k   853    50k     32   514   1.42  3   2   0    6 64  01946 22
 15   25k     0   25k   371   2034      2  1194   6.27  2   3   0    5 33  08503 21
 16   25k     0   24k   422    12k      0   443   3.72  7 3.3   0    4  2  3 618 26
 17   14k     4   14k   570    17k      5   634   3.97  1   2   0    5 53  0 11k 23

--------------------------------PATH STATS-----------------------------------
MoteA MoteB ABPower BAPower  ABTx(Fail)  ABRx  BATx(Fail)  BARx   Stab.
   1     6     -71     -74      0(   0)  5475  146k( 28k)  121k  80.67%
   1    13     -78     -82      0(   0)  3663  284k(186k)  103k  34.62%
   2    13     -76     -78   109k( 30k)   22k     0(   0)  1989  72.15%
   2    15     -88     -88      0(   0)   744   29k( 16k)   15k   44.2%
   2    17     -60     -67      0(   0)  1846   41k(4677)   10k  88.73%
   4    11     -86     -85   1183( 463)   103     0(   0)    37  60.86%
   4    15     -90     -88    745( 356)   405     0(   0)    32  52.21%
   6    14     -82     -84      0(   0)   209  9072(3428)   167  62.21%
  11    14     -81     -84   6681(2761)   454     0(   0)   144  58.67%
  11    16     -67     -67      0(   0)    54   727(  11)   134  98.49%
```

Figure. 7. Statistics of Network

3.2 Seven-hop experiment

Eight motes and a network manager were used for this experiment. As in the previous five-hop experiment, three parameters from the literature were used to measure the network performance: latency, stability, and reliability. We also studied the multihop stability of the path based on individual link stability values. Topological design was a deviation from industry best practices to study performance under strained condition. Due to the distance and obstacles among the motes and the network manager, latency, stability and reliability varied in each link. Average values were recorded for all three measurements throughout the network.

Latency

The average latency calculated by equations (1) and (2) is shown in Table 6.

Table 6: Average latency for each hop path

Number of Hops	Latency (in seconds)
1-hop Latency	0.328520661
2-hop Latency	0.607275862
3-hop Latency	1.106642857
4-hop Latency	1.82275
5-hop Latency	3.029172414
6-hop Latency	3.959137931
7-hop Latency	8.114444444

A hop-by-hop comparison of latency between the five-hop and seven-hop experiments reveal that the latency for seven-hop network is less than latency of five-hop network. Since there are more motes in the five-hop network, there are more data to be transferred throughout the network, which increase latency.

These findings show that communication over more than five-hops in WirelessHART standard is feasible and practical depending on the design of the topology.

Stability

The same equations (3) and (4) are used to compute stability values.

A snapshot of stability values for the experiment is shown in Fig 8 below. The first two rows show stability of the network manager with mote 2 and 5, which are directly connected to the network manager with stability values of 39.01% and 81.56% respectively. Stability for the link between mote 2 and network manager is less because of the mote's location outside the room. Some motes in this network have more than two neighbors, but only have good stability with one of them. Because WireleesHART supports graph routing, the motes choose the best route for the data to be transferred.

PATH STATS

MoteA	MoteB	ABPower	BAPower	ABTx(Fail)	ABRx	BATx(Fail)	BARx	Stab.
1	2	-80	-83	0(0)	4698	75k(45k)	32k	39.01%
1	5	-71	-65	0(0)	1726	155k(28k)	133k	81.56%
2	4	-72	-72	0(0)	979	43k(7582)	1148	82.41%
2	5	-66	-60	69k(5154)	3446	0(0)	788	92.56%
2	6	-91	-92	0(0)	12	964(797)	219	17.32%
3	6	-82	-83	15k(4850)	1719	0(0)	520	68.93%
3	13	-80	-83	5549(1333)	3196	0(0)	337	75.98%
3	17	-75	-83	0(0)	35	668(114)	262	82.93%
4	5	-92	-87	827(665)	149	0(0)	31	19.59%
4	6	-71	-70	0(0)	800	28k(3520)	1546	87.63%
4	13	-83	-84	0(0)	335	5856(1896)	3616	67.62%
6	13	-67	-68	0(0)	410	7019(471)	958	93.29%

Figure. 8: Stability values

Table 7 below summarizes average stability values for each hop path.

Table 7: Average stability for each hop path

Number of Hops	Stability
1 hop average Stability	81.56%
2 hops average Stability	87.06%
3 hops average Stability	85.51%
4 hops average Stability	86.04%
5 hops average Stability	87.44%
6 hops average Stability	85.57%
7 hops average Stability	85.19%

Again, comparing hop-by-hop stability values for both experiments, it was observed that seven-hop network has better average stability than its five-hop counterpart, which confirms the previous findings about the feasibility and practicality of more than five-hop communications in Wireless HART.

Reliability:

Same formula as in equation (5) is used to compute reliability.

NETWORK STATS

PkArr	PkLost	PkTx(Fail/ Mic/ Seq)	PkRx	Relia.	Latency	Stability
19k	1	74k(21k/ 0/ 0)	31k	99.99%	2.05s	71.63%

Figure. 9: Reliability Values

Reliability for this network is 99.99%. Even though latency has increased for this network compared to the five-hop network, it achieved better stability values. It takes longer for the data being transmitted to reach its destination but data loss was less.

Multihop Stability

We computed multihop stability from individual link stability values at discrete time slots over the entire lifespan of the experiment using (6). Table 8 below shows the reliability values.

Table 8: Multihop Stability for seven-hop experiment

Discrete time slots	Multihop Stability
1	31.94
2	24.38
3	13.85
4	15.24
5	17.8
6	17.33
7	14.7
8	14.88
9	22.34
10	21.85
11	23.93
12	23.88
13	21.8
14	14.45

4 Conclusion

We have conducted extensive experiments with multi-hop communications using WirelessHART in laboratory settings. Up to eight sensor motes were used for the experiments, which ran for months. Topologies were designed to provide five-hop and seven-hop communication paths designed to be run in two phases respectively. We have deliberately deviated from following the industry best practices in designing the topology to study network performance under strained conditions, which consist of single paths between motes. Network performance was measured using latency, stability, and reliability as defined in the WirelessHART literature. In addition, we have also studied network stability over multiple hops. The seven-hop network proved to have better results in terms of latency and stability, partly because of less number of motes used and the topology design. This shows the feasibility and practicality of multi-hop communications of Wireless HART beyond five-hop paths, given an efficient topology design.

We have found the reliability values of the five-hop and seven-hop networks in our chosen network configurations are still very close to 100%, 99.98% and 99.99%, respectively. These reliability values are based on the formula in the literature as shown in equation (5), which computes reliability without taking into account the effect of retransmissions. If packets need to be retransmitted, and eventually all retransmitted packets reach the network manager, reliability is computed as 100%. We have also studied multihop stability of the five-hop and seven-hop paths based on individual link stability values. As our topology design deviated from industry best practices, we have found that having at least one low stability link can have an impact on multihop stability, while still maintaining a very high overall network reliability of 99.98% or higher.

REFERENCES

[1] Chen, D., Nixon, M., Mok, A.: WirelessHART Real-time Mesh Network for Industrial Automation, Springer (2014).

[2] Gustafsson, D.: WirelessHART- Implementation and Evaluation of Wireless Sensors. Stockholm, Sweden (2009).

[3] I.E.C: Industrial communication networks - Wireless communication network and communication profiles - WirelessHART™, (2010).. Available: https://webstore.iec.ch/publication/7231. Accessed July 2016.

[4] IEEE: 802.15.4-2015 - IEEE Standard for Low-Rate Wireless Networks (2015). Available: https://standards.ieee.org/findstds/standard/802.15.4-2015.html. Accessed July 2016.

[5] Kim, A.N., Hekland, F. Peterson, S.: When HART goes wireless: Understanding and implementing the WirelessHART standard. In *IEEE International Conference on Emerging Technologies and Factory Automation*, 15-18 Sept (2008).

[6] Linear: SmartMesh WirelessHART. Linear Technology (2016). Available: http://www.linear.com/product/LTP5903-WHR. Accessed June 2016.

[7] Ngneoiepaye A., Tiam, Z.: Integrated Secure Heterogenous Wireless Sensor Network for Data Acquisition, Storage, and Presentation. Sr. Design paper, St Cloud, MN. (2015).

[8] Petersen, S. carlsen, S.: Performance Evaluation of WirelessHART for factory Automation. In *IEEE Conference on Emerging Technologies & Factory Automation*, Palma de Mallorca, Spain (2009).

[9] Raza, S., Voigt, T.: Interconnecting WirelessHART and Legacy HART. In *6th IEEE International Conference on Distributed Computing in Sensor Systems Workshops (DCOSSW)*, Santa Barbara, California, USA (2010).

[10] WirelessHART Technology Standard (2016). Accessed May 2016.

Society for Science and Education
United Kingdom

TNC Transactions on Networks and Communications

Volume 6, No. 1
ISSN: 2054 -7420

Outlier Resistant Time Series Operations via Qualitative Robustness and Saddle-Point Game Formalizations- A Review: Filtering and Smoothing

[1]P. Titsa Papantoni-Kazakos and [2]A.T. Burrell
[1]*University of Colorado Denver, Electrical Engineering Department, Denver, Colorado, USA*
[2]*Oklahoma State University, Computer Science Department, Stillwater, Oklahoma*
titsa.papantoni@ucdenver.edu; tburrell@okstate.edu; tosait@tutanota.com

ABSTRACT

Time series operations are sought in numerous applications, while the observations used in such operations are generally contaminated by data outliers. The objective is thus to design outlier resistant or "robust" time series operations whose performance is characterized by stability in the presence versus the absence of data outliers. Such a design is guided by the theory of qualitative robustness and is completed by saddle-point game formalizations. The approach is used for the development of outlier resistant filtering and smoothing operations.

Keywords: Time Series Analysis; Qualitative Robustness; Data Outliers; Filtering; smoothing.

1 Introduction

The fundamental desirable characteristic of outlier resistant or "robust: time series operations is performance stability; that is, a robust statistical procedure should guarantee small performance deviations for small perturbations in the data generating stochastic process. Thus, statistical robustness may be qualitatively defined along the latter lines, where for an analytical definition, the use of appropriate stochastic distance measures is essential. This qualitative definition is developed by the theory of *qualitative robustness*, while it also intimately related to the *robust saddle-point game theoretic formalizations.* The theory of qualitative robustness provides necessary conditions to be satisfied by robust operations, while the robust saddle-point game theoretic formalizations provide specific solutions within the qualitatively robust class of operations. In this paper, we will review this composite construction of statistically robust operations. We will then present solutions for outlier resistant or robust filtering and smoothing.

The definition of qualitative robustness was first given by Hampel (1971, who considered only memoryless data processes. The definition was extended to include processes with memory, first by Papantoni-Kazakos and Gray (1979) and then by Cox (1978), Bustos et al (1984) and Papantoni-Kazakos (1984a, 1984b, 1987). Solutions for outlier resistant prediction, filtering and smoothing were first developed by Tsaknakis et al (1988, 1986), while an overview of the theory can be found in Kazakos et al (1990). Extensions of the theory of qualitative robustness to include robust block encoders and quantizers were

DOI: 10.14738/tnc.61.2480
Publication Date: 05th March 2018
URL: http://dx.doi.org/10.14738/tnc.61.2480

developed by Papantoni- Kazakos (1981a, 1981b). Finally, a stochastic neural network was developed by Kogiantis et al (1997) and Burrell et al (1997), for implementation of robust prediction, and has been applied by Burrell et al (2012) for predictive model mapping.

The organization of the paper is as follows: In Section 2, we present the outline of the qualitative robustness theory and its relationship to robust saddle-point game theoretic formalizations. In Section 3, we describe the process for developing robust filtering operations. In Section 4, we draw from the derivations in Section 3, to develop non-causal filtering or smoothing operations, when the nominal information and noise processes are both Gaussian. In Section 5, we focus on robust causal filtering solutions for nominally Gaussian information and noise processes. In Section 6, we include concluding remarks.

2 Qualitative Robustness And Robust Saddle-Point Game Theoretic Formalizations

As discussed in the introduction, qualitative robustness corresponds to small performance deviations for small perturbations in the data generating processes. Alternatively, qualitative robustness is a continuity property defined on the space of stochastic processes via appropriate stochastic measures. In particular, let x^n and y^n denote n-dimensional data sequences, generated respectively by two non-identical n-dimensional probability density functions f_0^n and f^n. Let g(·) denote some function or operation on n-dimensional data sequences, where g(·) could be, for example, a test function in hypothesis testing or a parameter estimate. Let h_{0g} and h_g denote respectively the density function of the random variables $g(X^n)$ and $g(Y^n)$ (where X^n is generated by f_0^n, and where Y^n is generated by f^n), and let $\mathrm{d}_1(f_0^n, f^n)$ and $\mathrm{d}_2(h_{0g}, h_g)$ be two stochastic distance measures respectively between the densities f_0^n and f^n, and the densities h_{0g} and h_g. Then we can present the following definition,

Definition 1: The operation $g(\cdot)$ is qualitatively robust at the density function f_0^n, in stochastic distance measures $\mathrm{d}_1(\cdot,\cdot)$ and $\mathrm{d}_2(\cdot,\cdot)$, iff :

Given $\varepsilon > 0$, there exists $\delta > 0$ such that if f^n is such that $\mathrm{d}_1(f_0^n, f^n) < \delta$, then h_g is such that $\mathrm{d}_2(h_{0g}, h_g) < \varepsilon$.

From the above definition, we conclude that qualitative robustness is a local (around f_0^n) stability property, parallel to the continuity property of real function. The specific analytical properties of a qualitatively robust data operation $\mathrm{g}(\cdot)$ depend on the choice of the stochastic distance measures and $\mathrm{d}_1(\cdot,\cdot)$ and $\mathrm{d}_2(\cdot,\cdot)$. The latter stochastic distances are initially selected to best reflect the desired stability properties of the qualitatively robust data operation, where the weaker the distance $\mathrm{d}_1(\cdot,\cdot)$ and the stronger distance $\mathrm{d}_2(\cdot,\cdot)$, then the stronger the qualitative robustness properties. The main issue arising here is the relationship of the qualitative robustness to the robust saddle-point formalizations, and the choice of the stochastic distance measures $\mathrm{d}_1(\cdot,\cdot)$. We will first address the relationship to the robust saddle-point game-theory formalizations.

Let us consider a saddle-point game with payoff function f(x,y), where the function $f(\cdot,\cdot)$ and its arguments x and y are all real and scalar, and where x and y take values respectively in the subsets A and B of the real line R. Consider the metric d (*u* , *v*) = | *u* – *v* | on the real line, and let the subsets A and B both be convex with respect to that metric. Let at least one of those two subsets also be compact with respect to the metric $d(\cdot,\cdot)$, and let the payoff function f (x , y) be convex in x, concave in y, and continuous in x and y, with respect to the same metric. Then, the existence of a saddle-point solution (x^* ,y^*) such that $f(x^*, y) \le f(x^*, y^*) \le f(x, y^*)\,;\, \forall\, x \in A \text{ and } \forall\, y \in B$ is guaranteed and it is unique. If, on the hand, the function *f* (*x* , *y*) is not continuous in x and y, then the existence of a saddle-point solution is not generally guaranteed. The continuity of the payoff function is thus an essential property for the guaranteed existence of a saddle-point solution. The same is true when instead of x and y, we have density functions f^n and h_g as in Definition 1. In the latter case, the metric | *u* – *v* | on the real line is replaced by the stochastic distance measure $d_1(\cdot,\cdot)$ for the data generating densities f^n, and by the stochastic distance measure $d_2(\cdot,\cdot)$, for densities h_g induced by some f^n and some data operation *g*. Therefore, qualitative robustness is essential for the guaranteed solutions of the robust saddle-point game-theory formalization.

Let us now turn to the choice of the distances $d_1(\cdot,\cdot)$ and $d_2(\cdot,\cdot)$ in Definition 1. As we already pointed out, to make the qualitative robustness property strong, we need a weak distance $d_1(\cdot,\cdot)$ and a strong distance $d_2(\cdot,\cdot)$. A weak distance that also represents closeness in data sequences and best reflects the outlier model as well is the Prohorov distance [10], with data distortion measure $\rho_n(x^n, y^n)$ as follows.

$$\rho_n(x^n, y^n) = \begin{cases} n^{-1}\sum_{i=1}^{n}|x_i - y_i| = \gamma_n(x_1^n, y_1^n) & \text{if } n \text{ given and finite} \\ \inf\{\alpha : n^{-1}[\#i : \gamma_m(x_{i+1}^{i+m}, y_{i+1}^{i+m}) > \alpha] \le \alpha\} & \\ \qquad \text{if } n > n_0, \text{where } m \text{ and } n \text{ are postive integers} & \end{cases} \quad (1)$$

The Prohorov distance with data distortion measure as in (1) is a metric; that is, it satisfies the triangular property. For classes of memoryless processes, the distance is identical to the Prohorov distance with dtata distortion measure $\rho_1(x\ ,y\ ) = |x - y|$. Regarding the choice of the distance $d_2(\cdot,\cdot)$, the Vasershtein or Rho-Bar distances [10] are appropriate. Indeed, those two distances are strong and they both bound difference in expected error performance. The choice of the data distortion measure within the latter distances depends on the particular application, where a popular and useful such choice is the difference squared distortion measure $\rho^*(x\ ,y\ ) = (x-y)^2$. The Rho-Bar distance is used for closeness in stochastic processes. Given some data sequences $y_1^{N+n} = \{y_1, \ldots, y_{N+n}\}$ and some scalar operation $g(\cdot)$, let $g(y_i^{i+n})$ estimate the datum x_k of some process whose arbitrary dimensionality density function is f_2 and whose data sequence are …, x_{-1}, x_0, x_1 …. If the sequence y_1^{N+n} is generated by the density function f_0^{N+n}, let h_{0g} denote the arbitrary dimensionality density induced by f_0^{N+n} and the data operation g (·). Let h_g denote the arbitrary dimensionality density induced by g (·) and some other data density function f^{N+n}. Then, h_{0a} and h_a both estimate f_2. Given some data distortion measure $\rho(\cdot,\cdot)$, the goodness of those two estimates is respectively measured by the Rho-Bar distances $\bar{\rho}(f_2,h_{og})$ and $\bar{\rho}(f_2,h_g)$. If $\rho(u,v)=|u-v|$, then $\left|\bar{\rho}(f_2,h_{0g})-\bar{\rho}(f_2,h_g)\right| \le \bar{\rho}(h_{0g},h_g)$; thus, the Rho-Bar distance $\bar{\rho}(h_{0g},h_g)$ measures how closely h_{0g} fits f_2, as compared to the fitness of h_g to f_2. A similar conclusion is drawn, when the data distortion measure is the difference squared, $\rho^*(u,v)=(u-v)^2$ where then $\left|[\bar{\rho}^*(f_2,h_{0g})]^{1/2}-[\bar{\rho}^*(f_2,h_g)]^{1/2}\right| \le [\bar{\rho}^*(h_{0g},h_g)]^{1/2}$.

The definition of qualitative robustness, in conjunction with the Prohorov and Rho-Bar or Vasershtein distances lead to constructive sufficient conditions that data operations should satisfy [2], [6], [7] and [10]. These conditions are included in Theorem 1 below, whose proof can be found in [2].

Theorem 1 : Consider a scalar real operation $g(x^n)$ on data sequences x^n of length n. Let $g(x^n)$ be bounded, and such that :

i. If n is finite, then $g(x^n)$ is pointwise continuous as a function of the data. That is, given ε > 0, there exists δ > 0, such that $n^{-1}\sum_i |x_i - y_i| < \delta$ implies $\left|g(x^n)-g(y^n)\right| < \varepsilon$.

ii. If n is asymptotically large, and given some data generating density function f_0, then $g(x^n)$ is pointwise asymptotically continuous at f_0. That is, given ε > 0 and η > 0, there exist δ > 0, positive integers m and n_0, and for each $n > n_0$ some set A^n ε R^n, such that $\Pr(x^n \in A^n \mid f_0^n) > 1-\eta$ and $x^n \in A^n$ and $\inf\{\alpha : n^{-1}[\# i : \gamma_m(x_{i+1}^{i+m}, y_{i+1}^{i+m}) > \alpha] \le \alpha\} < \delta$ implies $|g(x^n)-g(y^n)| < \varepsilon \ \forall\, n > n_0$, where $\gamma_m(x_{i+1}^{i+m}, y_{i+1}^{i+m}) = m^{-1}\sum_{j=i+1}^{i+m} |x_j - y_j|$. Then the operation $g(\cdot)$ is qualitatively robust at the density function f_0^n, where in Definition 12.1.1, $d_1(\cdot,\cdot)$ is replaced by the Prohorov distance with data distortion measure as in (1) and $d_2(\cdot,\cdot)$ is replaced by either the Vasershtein or the Rho-Bar distances with distortion measure $\rho(u,v)$ equal either to |u – v| or some continuous function of | u – v|.

From Theorem 1, we conclude that to be qualitatively robust, it suffices that a data operation be bounded and continuous. For data sequences of finite length continuity is defined in the usual functional sense. For asymptotically large data sequences, continuity is defined as follows at some data generating density function: If some sequence x^n is representative of the latter density function, in the sense that it belongs to a high-probability set A^n, and if the majority of the elements of another sequence y^n are close to the corresponding elements of the sequence x^n, then the values $g(x^n)$ and $g(y^n)$ of the data operating are close as well. Due to the above results, we conclude that linear operations are not qualitatively robust. This is so because such operations are not bounded, and because closeness between the majority of corresponding elements of two sequences does not guarantee closeness in the values of those operations.

Qualitative robustness is a property that does not induce uniqueness. That is, given a specific problem, and some data generating density function f_0, there generally exists a whole class ϑ of data operations that are qualitatively robust at f_0. Additional performance criteria are thus needed, to evaluate and compare different data operations in class ϑ. Such performance criteria are the break-down point and the sensitivity, both defined asymptotically ($n \to \infty$) and at the density function f_0. Given f_0 and given some operation $g(\cdot)$ in class ϑ, consider the density functions f that are included in the Prohorov ball $\prod_{n,\rho_n}(f_0, f) \le \varepsilon$, where ρ_n is as in (1). Let h_{0g} and h_g be the density functions induced by the data operation $g(\cdot)$ and the densities f_0 and f respectively. Given some scalar data distortion measure $\rho(\cdot,\cdot)$, consider the Rho-Bar distance $\bar{\rho}(h_{0g}, h_g)$. Then, the *breakdown point* ε^*, of the operation $g(\cdot)$ at f_0 is the largest value ε, such that, if f is some density in the ball $\lim_{n\to\infty} \prod_{n,\rho_n}(f_0, f) \le \varepsilon$, then the distance $\bar{\rho}(h_{0g}, h_g)$ is a function of ε. The *sensitivity* of the operation $g(\cdot)$ at the density f_0 is defined as

$$\lim_{\substack{n\to\infty \\ \varepsilon\to 0}} \frac{\bar{\rho}(h_{0g}, h_g)}{\prod_{n,\rho_n}(f_0, f)}$$

It can be found that if bounded sensitivity at f_0 is required (parallel to bounded derivative) then the qualitatively robust operation $g(\cdot)$ should also be differentiable almost everywhere as a real function of the data, and for asymptotically large sequences it should be such that

$$| g(x^n) - g(y^n) | \le \text{c} \inf\{\alpha : n^{-1}[\#i : \gamma_m(x_{i+1}^{i+m}, y_{i+1}^{i+m}) > \alpha] \le \alpha\}$$

where *c* is some bounded constant, and where $x^n \in A^n$ for A^n as in part ii of Theorem 1 [see Papantoni-Kazakos (1984b)].

As may be deduced from the presentation in this section, qualitative robustness is a performance stability property and its time series applications include prediction, interpolation and filtering or smoothing. Solutions for the later time series operations require the marriage of qualitative robustness with the theory of saddle-point game theoretic formalizations. In this paper, we present such solutions for non-causal filtering or smoothing as well as for causal filtering.

3 Robust Filtering

The objective of either non-causal or causal filtering is the extraction of information carrying data from noisy observations. That is, the outcomes generated by an information process are estimated, when distorted by interferences from a noise process. We will assume that the relationship between the information and noise processes is additive. In the robust filtering problem, the information and noise processes are modeled by two disjoint classes, $\mathcal{F}_S$ and $\mathcal{F}_N$, respectively. Arbitrary dimensionality probability density functions in classes $\mathcal{F}_S$ and $\mathcal{F}_N$ are respectively denoted f_s and f_N.

Let f_{0S} and f_{0N} be two nominal well known, stationary density functions, such that $f_{0s} \in \mathcal{F}_S$ and $f_{0N} \in \mathcal{F}_N$. Let us assume that some density function f_s from class $\mathcal{F}_S$ is a priori selected by the system designer to represent the information process throughout the over all observation interval, and let us denote by …, X_{-1} , X_0, X_1, … a random data sequence generated by f_s . We initially assume that the class $\mathcal{F}_S$, consists of f_{0s} only.

Let us denote by …, W_{-1} , W_0, W_1, … random noise data sequences, and let …, Z_{-1} , Z_0, Z_1, … be data sequences from the nominal noise density function f_{0N} . Given some number ε_N in (0,1), let the class $\mathcal{F}_N$ of noise processes then be such that

$$W_n = (1-\varepsilon_N) Z_n + \varepsilon_N V_n \tag{2}$$

where …, V_{-1} , V_0, V_1, … is a random sequence generated by any arbitrary dimensionality stationary density function. The noise model in (2) represents the occurrence of outliers, with probability ε_N per datum. Given f_s in $\mathcal{F}_S$ and f_N in $\mathcal{F}_N$, we assume that the data sequences from f_s and f_N. are additive and that f_s and f_N. are mutually independent. Then, if …, Y_{-1} , Y_0, Y_1, … denote random observation sequences, we have,

$$Y_n = X_n + W_n \quad \forall n \tag{3}$$

where X_n is generated by f_s , W_n is generated by f_N [as in (2)], and the sequences …, X_{-1} , X_0, X_1, … and …, W_{-1} , W_0, W_1, … are mutually independent. Let $g_{n+l,F}(y_{-n}^{l-1})$ denote a filtering operation, estimating the information datum X_0 , via the observation sequence y_{-n}^{l-1} . Let $e_F(g_{n+l,F},\, f_s, f_N)$ denote the mean-squared error induced by the operation $g_{n+l,F}(y_{-n}^{l-1})$ + at the density functions $f_s \in \mathcal{F}_S$ and $f_N \in \mathcal{F}_N$. That is,

$$e_F(g_{n+l,F},\, f_s, f_N) = E\left\{\left[X_0 - g_{n+l,F}(Y_{-n}^{-1})\right]^2 \mid f_s, f_N\right\} \tag{4}$$

Consider then the following saddle-point game. Search for the triple $(g^*_{n+l,F}, f^*_s, f^*_N)$ such that $f^*_s \in \mathcal{F}_S$ and $f^*_N \in \mathcal{F}_N$ and

$$\forall f_s \in \mathcal{F}_S\,,\; f_N \in \mathcal{F}_N,\;\; e_F(g^*_{n+l,F}, f_s, f_N) \le e_F(g^*_{n+l,F}, f^*_s, f^*_N) \le e_F(g_{n+l,F}, f^*_s, f^*_N) \quad \forall\, g_{n+1,F} \tag{5}$$

The right part of (5) is satisfied for $g^*_{n+1,F}(y_{-n}^{l-1})$ being the conditional expectation of X_0 at f^*_s and f^*_N . That is

$$g^*_{n+1,F}(y_{-n}^{l-1}) = E\left\{X_0 \mid y_{-n}^{l-1}, f^*_s, f^*_N\right\} \tag{6}$$

The game in (5) reduces then to the following search. Find the pair (f^*_s , f^*_N) such that $f^*_s \in \mathcal{F}_S$ and $f^*_N \in \mathcal{F}_N$, and

$$E\left\{\left[X_0 - E\left\{X_0 \mid y_{-n}^{l-1}, f_s^*, f_N^*\right\}\right]^2 \mid f_s^*, f_N^*\right\} =$$

$$= \sup_{\substack{f_s \in F_s \\ f_N \in F_N}} E\left\{\left[X_0 - E\left\{X_0 \mid y_{-n}^{l-1}, f_s, f_N\right\}\right]^2 \mid f_s, f_N\right\} \tag{7}$$

and select $g_{n+l,F}^*(y_{-n}^{l-1})$ as in (6).

Given $f_s \in \mathcal{F}_s$ and $f_N \in \mathcal{F}_N$, and due to their additivity and mutual independence, the induced observation density f equals the convolution $f_s * f_N$, between the densities f_s and f_N. If μ_s and σ_s^2 denote respectively the mean and variance of the density f_s and defining then

$$\alpha(Y_{-n}^{l-1}) = \int_{R^{n-1}} dx_{-n}^{l-1}\, x_0\, f_s(y_{-n}^{l-1}) f_N(y_{-n}^{l-1}, x_{-n}^{l-1}) \tag{8}$$

we easily find, for $f = f_s * f_N$

$$E\left\{\left[X_0 - E\left\{X_0 \mid y_{-n}^{l-1}, f_s, f_N\right\}\right]^2 \mid f_s, f_N\right\} =$$

$$= \sigma_s^2 - \int_{R^{n+1}} dy_{-n}^{l-1} \frac{\left[\alpha(y_{-n}^{l-1}) - \mu_s f(y_{-n}^{l-1})\right]^2}{f(y_{-n}^{l-1})} \tag{9}$$

Let $\Phi_s(D_{-n},\ldots,D_{l-1},)$ and $A(D_{-n},\ldots,D_{l-1},)$ denote the characteristic functions (or Fourier transforms) at $\{D_i; -n \le i \le l-i\}$ of respectively the densities $f_s(y_{-n}^{l-1})$, $f_N(y_{-n}^{l-1})$, $f(y_{-n}^{l-1})$ and the function $\alpha(y_{-n}^{l-1})$ in (8), assuming that the former exist. Let us define the operator :

$$P(D_{-n},\ldots,D_{l-1}) = \frac{\frac{\partial}{\partial D_0}\Phi_s(D_{-n},\ldots,D_{l-1})}{\Phi_s(D_{-n},\ldots,D_{l-1})} \tag{10}$$

Then, the supremum in (7) reduces to the search of the infimum below, where $\mathcal{F}$ denotes the class induced by f_{0s} and f_N ; that is, $\mathcal{F} = \{f = f_{0s} * f_N,\ f_N \in \mathcal{F}_N\}$.

$$\inf_{f \in F} \int_{R^{n+1}} dy_{-n}^{l-1} \frac{\left\{P(D_{-n},\ldots,D_{l-1})\left[f(y_{-n}^{l-1})\right]\right\}^2}{f(y_{-n}^{l-1})} \tag{11}$$

We consider the class F_N of noise processes, as described by the probability density functions these processes induce and we select this class to be given by expression (12) below.

$$\mathcal{F}_N = \begin{array}{l}\{f : f = (1-\varepsilon_N) f_{0s} * f_{0N} + \varepsilon_N h \\ h \text{ is any arbitary dimensionality density function}\}\end{array} \tag{12}$$

We then express Theorem 2 below. This theorem and the subsequent Lemma 1 are due to Tsaknakis et. al. (1986).

Theorem 2 : Let the density f_{0s} have a nonzero and analytic characteristic function $\Phi_s(D_{-n},...,D_{l-1},)$ = $\Phi_s(\underline{D})$, that also admits a Taylor series expansion everywhere. Consider then the operator $P(\underline{D})$ = $P(D_{-n},...,D_{l-1},)$ in (10) which also admits then a Taylor series expansion. Consider the class $\mathcal{F}_N$ in (12), and denote

$$f_0 = f_{0s} * f_{0N} \tag{13}$$

Let $d(y_{-n}^{-1})$ be a positive solution of the equation

$$|P(\underline{D})d(y_{-n}^{l-1})| = \lambda\, d(y_{-n}^{l-1}) \quad \lambda > 0 \tag{14}$$

such that $d(y_{-n}^{l-1})$ is integrable over R^{n+1}, it is analytic for all nonzero vectors y_{-n}^{l-1}, and the quantity $P(\underline{D})[d*(y_{-n}^{l-1})]$ exists for all y_{-n}^{l-1} in R^{n+1}, where

$$d*(y_{-n}^{l-1}) = \begin{cases} (1-\varepsilon_N) f_0(y_{-n}^{l-1}) & \text{for } y_{-n}^{l-1} \in A^{n+1} \\ \lambda\, d(y_{-n}^{l-1}) & \text{otherwise} \end{cases} \tag{15}$$

where, A^{n+1} includes all y_{-n}^{l-1}, such that $|P(\underline{D})[f_0(y_{-n}^{l-1})]/f_0(y_{-n}^{l-1})| \le \lambda$.

Then, the infimum in (11) with substitution of $\mathcal{F}_N$ for $\mathcal{F}$, exists and is attained by the following density f^*

$$f*(y_{-n}^{l-1}) = d^*(y_{-n}^{l-1}) \tag{16}$$

with λ such that

$$\int_{R^{n+1}} f^*(y_{-n}^{l-1})\, d\, y_{-n}^{l-1} = 1 .$$

Furthermore, the filtering operation $g^*_{n+1,F}(Y_{-n}^{l-1})$ = $E\{X_0 \mid y_{-n}^{l-1}, f^*\}$ that satisfies (5) then the game in (5) on $\mathcal{F}_N$ is

$$g^*_{n+1,F}(y_{-n}^{l-1}) = \begin{cases} \dfrac{P(\underline{D})]f_0(y_{-n}^{l-1})]}{f_0(y_{-n}^{l-1})} & \text{for } y_{-n}^{l-1} \in A^{n+1} \\ \pm\lambda & \text{for } y_{-n}^{l-1} \in [R^{n+1} - A^{n+1}] \end{cases} \tag{17}$$

Lemma 1 below is a consequence of Theorem 2.

Lemma 1 : Let the densities f_{0s} and f_{0N} in Theorem 2 be both zero mean Gaussian, with respective auto-covariance matrices M_{n+1} and N_{n+1} , where the elements of M_{n+1} are denoted $\{m_{i,j}\}$.Then, the density f_0 in (13) is zero mean Gaussian, with auto-covariance matrix A_{n+1}= M_{n+1} + N_{n+1} and the density f^* in (16) and the filtering operator g^* in (17) take then the following special form, where | A_{n+1} | means determinant, T means transpose and (-1) denotes inverse, where it is assumed that Λ_{n+1} is nonsingular, and where $a_{n+1}^T = [m_{0,l-1},...,m_{0,-n}]$, $\operatorname{sgn} x = \{1\,; x \ge 0 \text{ and } -1; x < 0\}$.

$$f^*(y_{-n}^{l-1}) = \begin{cases} (1-\varepsilon_N)(2\pi)^{-(n-l)/2}|\Lambda_{n+1}|^{1/2}\exp\{-2^{-1}(y_{-n}^{l-1})^T\Lambda_{n+1}^{-1}y_{-n}^{l-1}\} \\ \qquad \text{for } y_{-n}^{l-1}: \left|a_{n+1}^T\Lambda_{n+1}^{-1}y_{-n}^{l-1} \le \lambda\right| \\ (1-\varepsilon_N)(2\pi)^{-(n-l)/2}|\Lambda_{n+1}|^{1/2}\exp\{-2^{-1}(y_{-n}^{l-1})^T\Lambda_{n+1}^{-1}y_{-n}^{l-1}\} \\ \quad + \dfrac{[\lambda - \left|a_{n+1}^T\Lambda_{n+1}^{-1}y_{-n}^{l-1}\right|]^2}{2a_{n+1}^T\Lambda_{n+1}^{-1}a_{n+1}} \qquad y_{-n}^{l-1}: \left|a_{n+1}^T\Lambda_{n+1}^{-1}y_{-n}^{l-1}\right| > \lambda \end{cases} \tag{18}$$

$$g_{n+1,F}^*(y_{-n}^{l-1}) = \begin{cases} a_{n+1}^T\Lambda_{n+1}^{-1}y_{-n}^{l-1} & \text{for } y_{-n}^{l-1}: \left|a_{n+1}^T\Lambda_{n+1}^{-1}y_{-n}^{l-1}\right| \le \lambda \\ \lambda\,\mathrm{sgn}(a_{n+1}^T\Lambda_{n+1}^{-1}y_{-n}^{l-1}) & \text{for } y_{-n}^{l-1}: \left|a_{n+1}^T\Lambda_{n+1}^{-1}y_{-n}^{l-1}\right| > \lambda \end{cases} \tag{19}$$

where denoting c = $\lambda[a_{n+1}^T\Lambda_{n+1}^{-1}a_{n+1}]^{1/2}$, and for $\phi(x)$ and $\Phi(x)$ denoting respectively the density at *x* and the cumulative distribution at *x* of the zero mean, unit variance Gaussian random variable, the constant λ is such that,

$$\Phi(c) + c^{-1}\phi(c) = 2^{-1}[1+(1-\varepsilon_N)^{-1}] \tag{20}$$

Given ε_N , *n* and *l*, the constant λ is positive and unique. Given *n* and *l*, λ decreases monotonically with increasing ε_N. For $\varepsilon_N = 0$, λ equals infinity, and the filtering operation in (19) becomes then identical to the optimal at the Gaussian noise, linear, mean-squared filter.

Denoting, $I(f\ ) = \int_{R^{n+1}} d\,y_{-n}^{l-1}\ f^{-1}(y_{-n}^{l-1})\{P(\underline{D})[f(y_{-n}^{l-1})]\}^2$, for the operator, $P(\underline{D})$, in (10), we also find $I(f^*)$ for density f^* in (18), where *c* is as in (20).

$$I(f^*) = 2(1-\varepsilon_N)\,a_{n+1}^T\Lambda_{n+1}^{-1}a_{n+1}[\Phi(c) - 2^{-1}] \tag{21}$$

We observe that the filtering operation is (19) is a truncated linear function of the data; it is thus bounded and continuous in the sense of part i in Theorem 1, but it is not asymptotically continuous in the sense of part ii in the same theorem. The latter operation is therefore qualitatively robust for finite data dimensionalities *n+l* only. We will extend the operation in (19), to create a filtering operation that is both asymptotically and non-asymptotically robust. We distinguish between casual and non-casual filtering, and we present then two different extensions.

4 Robust Non-Causal Filtering or Smoothing for Nominally Gaussian Information and Noise Processes

Consider the Gaussian densities f_{0s} and f_{0N} in Lemma 1. We then select some ε_N and some finite non-negative integer *m*. Let { …, X_{-1} , X_0, X_1, … } and { …, W_{-1} , W_0, W_1, … } denote sequences of random variables that are respectively generated by f_{0s} and f_{0N} . Given some integer *k* and some non-negative integer *n*, let

$N_{2n+1,k}$ and $M_{2n+1,k}$ denote respectively the auto-covariance matrices $E\{W_{k-n}^{k+n}(W_{k-n}^{k+n})^T \mid f_{0N}\}$ and $E\{X_{k-n}^{k+n}(X_{k-n}^{k+n})^T \mid f_{0s}\}$. Let $a_{2n+1,k}^T$ denote the (n+1) th row of the matrix $M_{2n+1,k}$, let $\Lambda_{2n+1,k} = M_{2n+1,k} + N_{2n+1,k}$, and let $g_{kl}^0(x_{k-n}^{k-l}, x_{k+l}^{k+n}); n \geq l$, denote the optimal mean-squared interpolation operation at the Gaussian density f_{0s} for the datum x_k, given x_{k-n}^{k-l} and x_{k-l}^{k+n}. Let us then define the sets $\{d_{k,n,l,j}; k-n \leq j \leq k-l, k+l \leq j \leq k+n\}$ and $\{b_{k,n,j}; k-n \leq j \leq k+n\}$ of coefficients as follows, where $\Lambda_{2n+1,k}$ is assumed non-singular.

$$\{d_{k,n,l,j}\}: g_{kl}^0(x_{k-n}^{k-l}, x_{k+l}^{k+n}) = \sum_{j=k-n}^{k-l} d_{k,n,l,j} x_j + \sum_{j=k+l}^{k+n} d_{k,n,l,j} x_j \tag{22}$$

$$[b_{k,n,k-n},\ldots,b_{k,n,k+n}] = a_{2n+1,k}^T \Lambda_{2n+1,k}^{-1}$$

Let us now define

$$g_n^s(x) = \begin{cases} x & \text{if } |x| \leq \lambda_n \\ \lambda_n \operatorname{sgn}(x) & \text{otherwise} \end{cases} \tag{23}$$

where $c = \lambda[a_{2n+1,k}^T \Lambda_{2n+1,k}^{-1} a_{2n+1,k}]^{-1/2}$ is such that

$$\Phi(c) + c^{-1}\phi(c) = 2^{-1}[1 + (1-\varepsilon_N)^{-1}] \tag{24}$$

Let $\hat{x}_{k,n}^s$ denote the estimate of the signal datum x_k from the observation vector y_{k-n}^{k+n}.

Then the estimate $\hat{x}_{k,n}^s$ is designed as in (25) below, where it can be shown that it is qualitatively robust both non-asymptotically and asymptotically.

$$\hat{x}_{k,n}^s = \begin{cases} g_n^s(a_{2n+1,k}^T \Lambda_{2n+1,k}^{-1} y_{k-n}^{k+n}) & \text{if } n \leq m \\ g_{kl}^0(\hat{x}_{k-n}^{k-1}, \hat{x}_{k+1}^{k+n}) & n > m \end{cases} \tag{25}$$

where $\hat{x}_j^i = [\hat{x}_{j,m}^s, \ldots, \hat{x}_{i,m}^s]; i > j$ and $g_{kI}^0(\cdot)$ is as in (22).

Let us define

$$r_n^s(n) = a_{2n+1,k}^T \Lambda_{2n+1,k}^{-1} a_{2n+1,k} \tag{26}$$

Then, $r_k^s(n)$ represents a variance gain in estimating the signal datum x_k from the observation vector y_{k-n}^{k+n} at the zero mean Gaussian noise density whose auto-covariance matrix is as in (22). Therefore, $r_k^s(n)$ is monotonically non-decreasing with increasing n. Given ε_N, the same monotonicity characterizes the truncation constant λ_n in (23), whose maximum value λ_∞ equals $c \lim_{n\to\infty}[r_k^s(n)]^{1/2}$, where c is the solution of (24). If the densities f_{0s} and f_{0N} are both stationary, with respective power spectral densities, $p_{0s}(\lambda)$ and $p_{0N}(\lambda)$; $\lambda \in [-\pi, \pi]$ and if $m \to \infty$, then directly from (19) we obtain

$$\lambda_\infty = c[E\{X_0^2 \mid f_{0s}\} - e_F(p_{0s}, p_{0N}]^{1/2}$$

$$= c\{(2\pi)^{-1}\int_{-\pi}^{\pi} p_{0s}(\lambda)\,d\lambda - (2\pi)^{-1}\int_{-\pi}^{\pi} p_{0s}(\lambda)[p_{0s}(\lambda)+p_{0N}(\lambda)]^{-1} p_{0N}(\lambda)d\lambda\}^{1/2}$$

$$= c\{(2\pi)^{-1}\int_{-\pi}^{\pi} p_{0s}^2(\lambda)[p_{0s}(\lambda)+p_{0N}(\lambda)]^{-1}d\lambda\}^{1/2}$$

5 Robust Causal Filtering for Nominally Gaussian Information and Noise Processes

Given the Gaussian densities f_{0s} and f_{0N} in Lemma 1 and the sequences { ..., X_{-1} , X_0, X_1, ... } and { ..., W_{-1} , W_0, W_1, ... }of random variables as in the non-causal filtering, let $M_{n,k}$ and $N_{n,k}$ denote respectively the auto-covariance matrices $E\{X_{k-n+1}^k (X_{k-n+1}^k)^T \mid f_{0s}\}$ and $E\{W_{k-n+1}^k (W_{k-n+1}^k)^T \mid f_{0N}\}$, where n ≥ 0 . Let then $a_{n,k}^T$ denote the first row of the matrix $M_{n,k}$, and let $\Lambda_{n,k} = M_{n.k} + N_{n,k}$. Let $g_{kl}^0(x_{k-n+1}^{k-l}), n-1 \geq l$, denote the optimal mean-squared prediction operation at the Gaussian density f_{0s} for the datum x_k , given x_{k-n+1}^{k-l} . Assuming that $\Lambda_{n,k}$ is nonsingular, let us then define the sets $\{c_{k,n-1,l,j}\, ; k-n+1 \leq j \leq k-l\}$ and $\{h_{k,n,j}\, ; k-n+1 \leq j \leq k\}$ of coefficients as

$$\{c_{k,n-1,l,j}\} : g_{kl}^0(x_{k-n+1}^{k-l}) = \sum_{j=k-n+1}^{k-l} c_{k,n-1,l,j}\, x_j \tag{27}$$

$$[h_{k,n,k-n+1}, \ldots, h_{k,n,k}] = a_{n,k}^T \Lambda_{n,k}^{-1}$$

Let us now define

$$g_n^c(x) = \begin{cases} x & \text{if } |x| \leq \mu_n \\ \mu_n \operatorname{sgn}(x) & \text{otherwise} \end{cases} \tag{28}$$

where $c = \mu\,[a_{n,k}^T \Lambda_{n,k}^{-1} a_{n,k}]^{-1/2}$ is such that

$$\Phi(c) + c^{-1}\phi(c) = 2^{-1}[1 + (1-\varepsilon_N)^{-1}] \tag{29}$$

Let $\hat{x}_k^c(n)$ denote the estimate of the signal datum x_k from the observation vector y_{k-n+1}^k . Then, the estimate $\hat{x}_k^c(n)$ is designed as follows, where ε_N and *m* are a priori selected.

$$\hat{x}^{c}_{k,n} = \begin{cases} g^{c}_{n}(a^{T}_{n,k}\,\Lambda^{-1}_{n,k}\,y^{k}_{k-n+1}) & \text{if } n \le \text{m} \\ \sum_{j=k-n+1}^{k-m} c_{k,n-1,m,j}\,\hat{x}^{c}_{j,\,j+n-k} & \\ + g^{c}_{m}\left(\sum_{\text{j=k-m+1}}^{\text{k}} h_{k,n,j}[y_j - g^{0}_{jp}(\hat{x}^{j-m}_{k-n+1})]\right) \;; & \text{if } n > m \end{cases} \quad (30)$$

Where $g^{0}_{jp}(\cdot)$ is as in (27) , and where $\hat{x}^{i}_{j} = [\hat{x}^{c}_{j,j+n-k}, \ldots, \hat{x}^{c}_{i,i+n-k}]$.

Let us define,

$$r^{c}_{k}(n) = a^{T}_{n,k}\,\Lambda^{-1}_{n,k}\,a_{n,k} \quad (31)$$

Then, $r^{c}_{k}(n)$ represents the variance gain in estimating the datum x_k from the observation vector y^{k}_{k-n+1} at the zero mean Gaussian density, whose auto-covariance matrix is as in (27). Thus, $r^{c}_{k}(n)$ is monotonically non-decreasing with increasing n, and so is then the truncation constant μ_n in (27), where ε_N remains fixed.

It can be shown [Tsaknakis (1986)] that the operations in (30) are qualitatively robust, in both the asymptotic and the non-asymptotic sense. In the later operation, the integer *m* and ε_N represent a tradeoff between optimality at the Gaussian noise f_{0N} density robustness, and they are both system parameters. As *m* increases and ε_N decreases, the filtering operation in (30) tends to the optimal at the Gaussian density f_{0N}, linear data operation.

6 Conclusions

We have examined outlier resistant time series operations in the light of the theory of qualitative robustness. The resulting operations are continuous, both in a pointwise and an asymptotic sense, as well as bounded. Their performance is controlled by two parameters, one of which represents outlier contamination level. Special attention has been given to causal and non-causal filtering.

REFERRENCES

[1] Hampel, F.R. (1971). A General Qualitative Definition of Robustnes. *Ann. Math. Statist.* 42, 1887-1895.

[2] Papantoni-Kazakos, P. and R.M. Gray (1979). Robustness of Estimators on Stationary Observations. *Ann. Prob.* 7, 989-1002.

[3] Cox, D (1978). Metrics on Stochastic Processes and Qualitative Robustness. *Tech. Report No. 23.* Dept. of Staistics, Univ. of Wash., Seattle.

[4] Bustos, O., R. Fraiman and V. Yohai (1984). Asymptotic Behavior of the Estimates Based on Residual Autocovariances for ARMA Models. Robust and Nonlinear Time Series Analysis in *Lecture Notes in Statistics.* Springer-Verlag, New York, 26-49.

[5] Papantoni-Kazakos, P. (1984a). A Game Theoretic Approach to Robust Filtering. *Information and Control* 60, Nos. 1-3, 168-191.

[6] Papantoni-Kazakos, P. (1984b). Some Aspects of Qualitative Robustness in Time Series. Robust and Nonlinear Time Series Analysis in *Lecture Notes in Statistics.* Springer-Verlag, New York, 218-230.

[7] Papantoni-Kazakos, P. (1987). Qualitative Robustness in Time Series. *Information and Computation* 72, No. 3, 239-269.

[8] Tsaknakis, H. and P. Papantoni-Kazakos (1988). Outlier Resistant Filtering and Smoothing. *Information and Computation* 79, 163-192.

[9] Tsaknakis, H., D. Kazakos and P. Papantoni-Kazakos (1986). Robust Prediction and Interpolation for Vector Stationary Processes. *Prob. Th. And Related Fields* 72, Springer-Verlag, New York, 589-602.

[10] Kazakos, D. and P. Papantoni-Kazakos (1990). Detection and Estimation. *Computer Science Press,* New York.

[11] Papantoni-Kazakos, P. (1981a). Sliding Block Encoders that are Rho-Bar Continuous Functions of Their Input. *IEEE Trans. Inf. Theory,* IT-27, 372-376.

[12] Papantoni-Kazakos, P. (1981b). Stochastic Quantization for Performance Stability. *Information and Control* 49, No. 3, 171-198.

[13] Kogiantis, A. and P. Papantoni-Kazakos (1997). Operations and Learning in Neural Networks for Robust Prediction. *IEEE Trans. Systems, Man and Cybernetics* 27, No. 3, 402-411.

[14] Burrell, A.T., A. Kogiantis and P. Papantoni-Kazakos (1997). Detecting Changes in Acting Stochastic Models and Model Implementation via Stochastic Neural Networks. *Statistical Methods in Control and Signal Processing*. Editors: S. Sugimoto and T. Katayama. Marcel Dekker.

[15] Burrell, A.T. and P. Papantoni-Kazakos (2012). Stochastic Binary Neural Networks for Qualitatively Robust Predictive Model Mapping. *International Journal of Communications Network and System Sciences (IJCNS).* Special Issue on Models and Algorithms for Applications, September, Vol. 5, 603-608.

SOCIETY FOR SCIENCE AND EDUCATION
UNITED KINGDOM

TNC TRANSACTIONS ON NETWORKS AND COMMUNICATIONS

VOLUME 6, NO. 1
ISSN: 2054 -7420

Isolation of Water Inflow to Production Wells

Ahmetkaliev R.B., PhD, Zhangissina Gulnur D., PhD, Professor,
Nasibullin B.M., PhD, Bahtigereev A.R.,
Almaty University of Energy and Communication(Almaty, Kazakhstan)
gul_zhd@mail.ru

The analysis of dehydration of water-in-oil emulsion from dispersed content is carried out. It is shown that the dispersed system has the connection with drops water-in-oil emulsion and its influence on viscosity and on stability these systems.

The process of formation and transformation of oil-water emulsions in situ and using them to isolate the water inflow to the production wells. The existence of a bond between droplets and a dispersion medium and its effect on the stability and viscosity of an oil dispersed system is shown. One of the effective methods for maintaining reservoir pressure is the flooding of seams, which can ensure high rates of development and achievement of maximum oil recovery.

The process of oil extraction from oil-bearing strata is accompanied by continuous mixing of oil with water and formation of water-oil emulsions (VNE). This process occurs when lifting watered oil from the bottom of the wells to its mouth and further in the fishing lines. The mixing of oil with water and the formation of NOE often occurs already in reservoir conditions in the process of oil displacement by water. In the near-wellbore zone of the well (CCD), the movement of the emulsion occurs under pressure-reducing conditions. A decrease in the pressure in the liquid occurs also when it rises to the wellhead.. The change in the thermobaric conditions is facilitated by the partial separation of the gas components of the oil, the formation of microdispersions from high-molecular compounds. The latter can be sorbed on the surface of water droplets in the emulsion, deposited on the walls of the collectors in the CCD, on the walls of pipes transporting oil. On the surface of water droplets, natural stabilizers of emulsions, available in oil, are also sorbed. As a result of these sorption and hydrodynamic processes, the dispersed composition changes in the direction of decreasing the size of the water droplets and increases the stability of the emulsion /1-4 /.

The water content in oil can reach significant values. The process of watering the wells worsens the state of development of the field. Restriction of water inflow is a problem not only of technological nature, but also directly related to oil recovery of reservoirs.

There are various methods of isolating the water inflow to producing wells: polymer and silicate-gel technology, foam technology, sedimentation, isolation using reverse-type water-oil emulsions (1-4). The aim of the research is to conduct a series of laboratory filtration experiments and determine the effectiveness of using nanoclay to improve the mechanical properties of gels and VNE used in insulation work. To prepare grouting mortars, liquid glass and hydrochloric acid were used. An aqueous solution of

DOI: 10.14738/tnc.61.4196
Publication Date: 14th March 2018
URL: http://dx.doi.org/10.14738/tnc.61.4196

hydrochloric acid and liquid glass has the property of forming a gel for a period of time, which depends on the concentration of these components.

We conducted experiments using the following composition: liquid glass 3%, hydrochloric acid 0.66%, laponite 1%. The result of the experiment is shown in Figure 1.

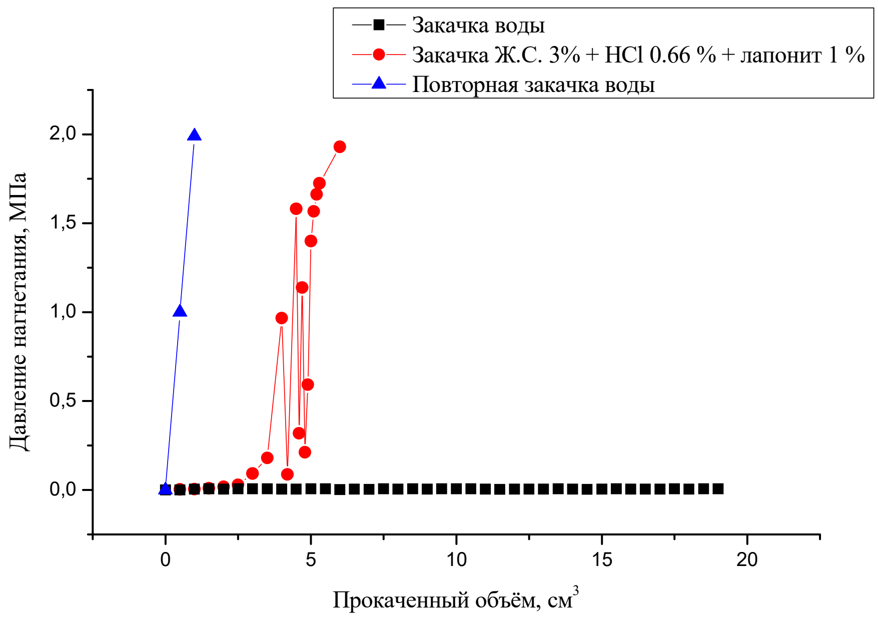

Figure.1. Change in discharge pressure before injection of a solution of liquid glass (3%) + HCl (0.66%) + laponite 1% and with repeated water pumping.

It can be seen from the above figure that when the concentration of laponite was reduced, it was possible to pump a larger volume of a grouting mortar. Re-injection of water led to a sharp increase in injection pressure up to 2 MPa. Such discharge pressure values were not achieved in the two previous experiments. In addition, it can be seen from the figure that a decrease in the concentration of laponite from 6 to 1% allowed pumping the volume of a grouting mortar in the bulk layer equal to 60% of the pore volume.

It should also be noted that when the water was re-injected, there was no displacement of the gel phase from the model. This indicates that the mechanical properties of the gel have been improved by adding laponite to it. The increase in the mechanical properties of the gel led to a decrease in the permeability of the model in this case approximately 400 times. Thus, the results of the experiments showed that using liquid glass, hydrochloric acid and laponite, it is possible to select an optimal solution formulation that will reduce the permeability of the porous medium by 400 or more, which allows us to cover the majority of the bottomhole zone of the well (Fig.1).

In field conditions, VNE is prepared on the surface to create a water-insulating barrier and it is injected into the treated formation through the production well. Under certain conditions, the water-oil emulsion for this purpose can be prepared directly in the productive layer using electric and acoustic methods. The method of electric effect is based on the phenomena of the change in permeability of the filtrate (water and oil) and the change in the filtration properties of the medium when electric current is passed through it in special modes. When the electric current passes through the reservoir, the following physical phenomena occur:

- heating and cooling the fluid in the narrow places of the pore channels of the rock, which leads to cyclic, sharp pressure drops and will facilitate the separation of resin-asphaltene deposits from the walls of pore channels into the oil and water phase;

- thermoplastic stresses arising as a result of various thermal and electrical parameters of the rock and fluid, which will also contribute to the separation of resin-asphaltene deposits;

- Processes of heating the medium while passing a current through the rock will be accompanied by the release of gas from the oil and the evaporation of water, which result in an increase in pressure and the formation of shock waves.

These phenomena occur more intensively in capillaries filled with water, in "more oil capillaries" these processes occur to a lesser degree.

The formation of resin-asphaltene deposits on the walls of the pore channels occurs when oil is filtered through them. This is accompanied by a decrease in their permeability, which manifests itself more in less permeable reservoirs. From more permeable reservoirs, oil separates faster and through these channels the intensive flow of water to production wells begins.

When heated or otherwise exposed, resin-asphaltene deposits are separated from the walls of the collectors, dispersed and form water-oil emulsions with high aggregative and sedimentation resistance. The emulsions formed have a viscosity much greater than oil and water. Their filterability through the pore channels is very small, so the flow of such VNE is directed to higher permeable pores and they are clogged. This leads to a redistribution and equalization of the oil injection profile, oil recovery increases.

The treatment was carried out by the method of electric impact on 34 wells of the Uzen deposit. The following results were obtained:

Success in reducing water cut 85%, increasing oil production by 94%, watercut decreased by an average of 9%, oil production increased by 3.2 tons per day.

The change in the stability of VNE in reservoir conditions can occur with other physical impacts on the productive formation of the bottomhole well zone. This is an acoustic action in which a high-intensity sound wave cleans the collector walls in the CCD from the AFS and other deposits / 3 /.

The method of acoustic impact is based on the phenomena of the change in the permeability of the filtrate (water and oil) and the change in the filtration properties of the medium. The oil reservoir is represented by both solid and liquid phases, in it there is a complex combination of interaction between longitudinal and transverse fields. Under the influence of a longitudinal wave, the filling fluid tends to move toward the pressure drop, flowing into adjacent pores, while at the same time as the shear stresses of the solid skeleton of the collector impart a torque to the fluid. Thus, the fluid movement occurs as a vortex flow, which performs intensive reciprocating movements. These processes determine the nature of fluid motion in the pores of the formation. Acoustic waves are reflected from the walls of the collectors, which leads to the imposition of the incident and reflected waves, the formation of standing waves. The amplitude of the pressure fluctuation within the limits of the wavelength in these sections increases approximately by a factor of two. Such zones are formed at the walls of the collectors.

With acoustic impact on the reservoir, the following physical phenomena occur:

- the vortex reciprocating motion of the filtrate in the narrow places of the pore channels of the rock, which leads to cyclic, sharp pressure drops and will promote the mixing of water and oil with the formation of a water-oil emulsion (VNE);
- These same processes will lead to the separation of resin-asphaltene deposits from the walls of pore canals and their transfer to the oil and water phase, which increase the stability of the formed VNE.

The treatment was carried out by the method of acoustic influence on 3 wells. The following results were obtained:

Success in reducing water cut 100%, increasing oil production by 100%, watercut decreased by an average of 11%, oil production increased by 2.2 tons per day.

We have developed another version of the restriction of water inflow to producing wells.

To improve the technological characteristics of liquid hydrocarbons, other variants of wave and electromagnetic effects can also be used (3,4).

7 Literature

[1] Innovative patent of the Republic of Kazakhstan № 29428 "The method of isolation of washed high permeability zones of the productive layer" // Bulletin of inventions of the Republic of Kazakhstan № 12, 2014. Akhmetkaliev R.B., Nasibullin B.M., Akhmetkaliev A.R.

[2] Innovative patent of the Republic of Kazakhstan № 29858 "The way of isolation of washed high permeability zones of the productive formation" // Bulletin of inventions of the Republic of Kazakhstan №5, 2015. Akhmetkaliev R.B., Nasibullin B.M., Akhmetkaliev A.R.

[3] R.Akhmetkaliev. Formation and transformation of water-oil emulsion // Journal "Search", a series of natural and technical sciences, No. 1 (2), 2014, pp. 80-85.

[4] Akhmetkaliyev R.B. Processes of transformation of water-oil emulsion and oil dispersed system // Journal of Higher School of Kazakhstan, No. 1 (1), 2017, pp. 60-65.